This paper first appeared in the eleventh print edition of *Photovoltaics International* journal, published in February 2011.

Challenges of the wire saw wafering process

Thomas Behm, **Wolfgang Fütterer**, **Claudia Funke**, **Steffi Kaminski**, **Hans-Joachim Möller**, **Romy Rietzschel** & **Thomas Wagner**, TU Bergakademie Freiberg, Institute of Experimental Physics, Freiberg, Germany

ABSTRACT

This paper discusses the wire sawing process and its impact on the wafer surface and subsurface. Surface damage is found to be the main determinant in wafer stability, while an outline of the sawing parameters that have a strong influence on the surface and subsurface damage is presented. The results indicate how it is possible to decrease the breakage rate of wafers and improve the homogeneity (e.g. TTV) of wafer surfaces. A further goal in the development of the wire sawing process is to successfully reduce material consumption. This can be achieved by sawing thinner wafers with thinner wires, which leads to a reduction of the kerf loss per produced silicon surface. The second option is to increase the material yield by decreasing the wafer breakage. It will be shown that silicon wafers with less and shorter cracks and smoother surfaces will give a higher yield, while proceeding to discuss some of the important factors that affect the microcrack formation.

Introduction

Multi-wire sawing still remains the main slicing technique for large multi- and monocrystalline silicon crystals in the photovoltaics and microelectronics industries. Since sawing contributes considerably to the wafer production cost, there is a great level of incentive to improve the sawing technique for further cost reduction in mass production. Slurry-based sawing is still the main technique used today, but sawing with fixed abrasive wires is an option for the future. Research actions and results of various groups over the last few years have led to a basic understanding of the microscopic details of the slurry-based sawing process, some of which are important to the focus of this paper. Advances in the wafer production process towards thinner wafers, higher yield, lower consumption of energy and consumables has shifted the focus to new issues.

These issues – many of which will be addressed here – have been investigated and developed using new experimental techniques by TU Bergakademie Freiberg over the last few years. For this purpose, an industrial wire saw was equipped with monitoring tools such as force and temperature sensors and a high-speed camera, allowing our researchers to obtain more of an insight into the microscopic details of the sawing process and the interaction processes of the wire, the slurry fluid and SiC particles with the silicon crystal.

Slurry-based multi-wire sawing experiments were performed under different conditions to investigate the influence of machine and material parameters on the sawing process and wafer quality. Important parameters like wire thickness and feed and wire speed were changed, while a range of slurry types were used, allowing the variation of such features as silicon carbide grain size, carrier fluids and silicon carbide loads. The as-sawn wafers were characterized by determining the fracture stress distribution, the surface roughness and subsurface damage, and the thickness variations (TTV) of the wafers. The results can be analyzed with respect to the factors that are important for further improvement of the slurry system, the wires and the sawing parameters.

Microscopic removal process of rolling and indenting particles

There is a general consensus that free-floating abrasive particles in the sawing channel remove material by rolling and indenting into the silicon crystal surface, the basic mechanism behind which is described in the following. SiC powders are currently mainly used as an abrasive; diamond powders are also an option but are not used in mass production for obvious cost reasons. In order to ensure good lubrication in the sawing channel, the particles have to be suspended in a carrier fluid, the most commonly used being polyethylene glycol (PEG). However, the role of the fluid and its relevant properties are still not completely understood.

The abrasive slurry is introduced above the wire web. This wire web then drags the slurry to the silicon ingot, which is moved toward the wire web at a feed rate of 0.4 to 0.8mm/min. The wire moves at a speed of up to 15m/s.

A closer look at the sawing channel is necessary in order to thoroughly analyse the removal process. The schematic in Fig. 1, which depicts events in the sawing channel, shows a situation whereby the silicon is being pushed bottom-up against the wire. The space between the wire and the crystal surface is filled with the carrier fluid and abrasive particles. The coarser particles are in contact with the wire and the silicon surface. As the wire pushes against the particles, it indents these particles in the silicon surface. Those particles between the wire and the ingot are mainly responsible for the material removal process, whereas the particles at the side of the channel determine the damage on the final wafer surface.

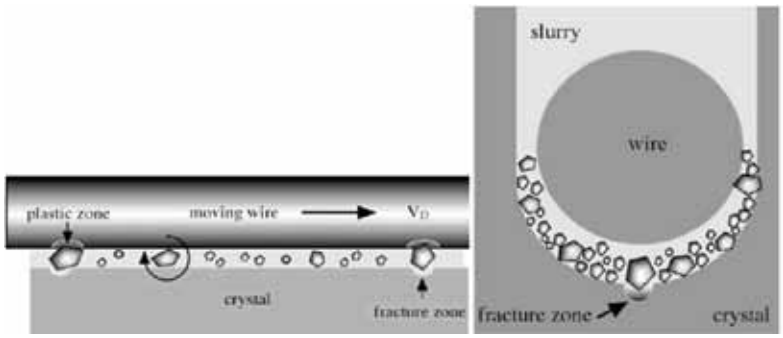

Figure 1. Left: Schematic diagram of wire, slurry with abrasive, and crystal in the cutting zone. Under external force the wire bows and exerts forces on the particles and the slurry fluid. Right: Cross section of wire, slurry with abrasive, and crystal in the cutting zone [1].

Indentation pattern

The interaction between the abrasive SiC particles and the crystal yields a distinct damage pattern on the surface that can be analyzed using microscopic techniques. The typical surface structure consists of local indentations (Fig. 2) with a mean diameter of a few micrometers. A single indentation by a Vickers-indenter provides a good model of a single chipping event.

The structure of the wafer's surface, as shown in Fig. 3, can be explained by the indentation of loose, rolling particles into the crystal surface, which eventually chips away small silicon pieces. Since SiC particles are facetted and contain both sharp edges and tips, they can exert high local pressures on the surface. This rolling-indenting grain model forms the physical basis of our description of the wire sawing process.

Median cracks are generated as well as the abrasion by lateral cracks. These median cracks extend into the bulk material and are unavoidable in terms of the use of the wire saw technique (Fig. 4).

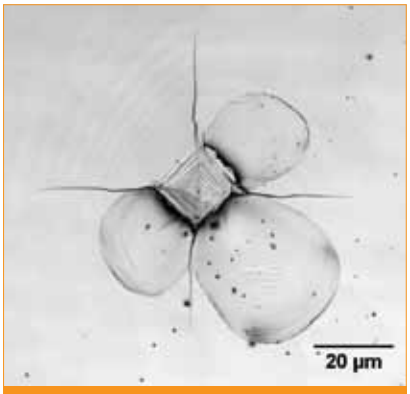

Figure 2. Damage structure after an isolated Vickers indentation. Material is removed by chipping under the load.

Figure 3. Surface of slurry wire sawn silicon wafer.

In-situ observations of abrasive particles

In the quest for evidence of the rolling and indenting particle process, a new method has been established that provides a direct glimpse into a sawing channel [2]. This model experiment involves the cutting of a steel wire into a transparent glass brick, giving a clear view of the rolling and indenting processes in the glass body by using a high-speed camera combined with a microscopic objective.

For the purposes of analysis, a glass ingot with a prepared sawing channel was fixed into a laboratory single wire saw, with the sawing channel located close to the camera side of the glass surface. A cutting wire with a diameter of 120µm was introduced into the prepared sawing channel. The slurry consists of PEG 300 and SiC with an F800 particle size of d50 = 6.5µm and a very diluted slurry with a load of 2 wt. % [3]. This low slurry load was necessary to allow the observation of distinguishable particles. The single wire loop was 75cm long with a speed between 2mm/s and 2m/s. A high-speed camera, which can take up to 30,000 pictures per second, was combined with a microscopic objective with a 10- to 63-fold magnification so that the motion of individual particles was rendered observable.

Fig. 5 presents a lateral view into the sawing channel, including the visible silicon carbide particles (black dots) below the wire where the chipping takes place. The measured height between the wire and the ingot surface is about 10 to 16µm and is determined by the size of the bigger particles. The upper part of the image shows the already-cut glass ingot as well as particles that have been flushed upwards along the side of the wire.

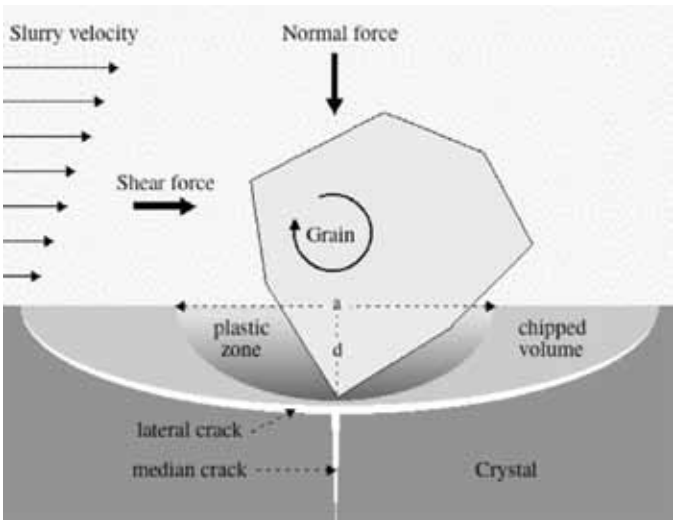

Figure 4. Schematic indentation of a particle into a brittle substrate. Under the action of normal and shear forces, first a plastic zone and then two crack systems are formed. The extension of the lateral cracks and the depth of the plastic zone give an approximate determination of the chipped volume. The median cracks partially remain in the subsurface and are part of the saw damage.

The biggest particles were found to come into contact with both the wire and the crystal surface; those particles that touch the moving wire rotate in the sawing channel (Fig. 6), which is clearly visible in images taken from a time sequence of the process in the sawing channel. The particle in the middle of the sawing channel rotates in the same direction as the wire moves as a result of contact by the wire, while the single edges of the particle are made to spin by the particle's rotation. This special particle has a low circularity.

The results confirm that cutting is carried out by particles in contact with both the wire and ingot. It also appears that the biggest particles can be removed from the sawing channel either at the wire inlet or by squeezing them sideways out of the cutting zone.

Measured parameters

The formation of cracks and therefore the removal process depends on machine parameters such as wire and feed speed, and the slurry properties [4]. Force measurements at the ingot are a useful tool for the evaluation of the impact of these parameter variations.

Force measurements during wire sawing

A silicon ingot might be lost when the wire ruptures during cutting, an error that can be avoided by reducing the tension on the wire. The total tension consists of the wire tension given by the machine and the additional tension caused by the force of the brick. Measurement of the

Figure 5. Image of the sawing channel in a glass sample as viewed from the side. The channel is illuminated from the back side with a halogen lamp. The particle movement was observed with a high-speed camera [2].

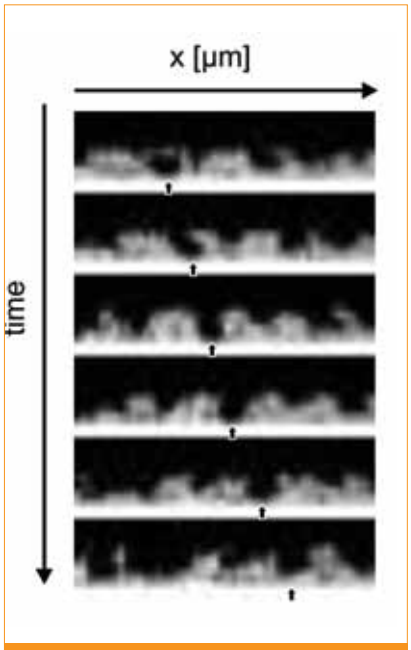

Figure 6. Successive images of the sawing channel in a glass sample showing the rotation of a single SiC particle (section width is 137µm).

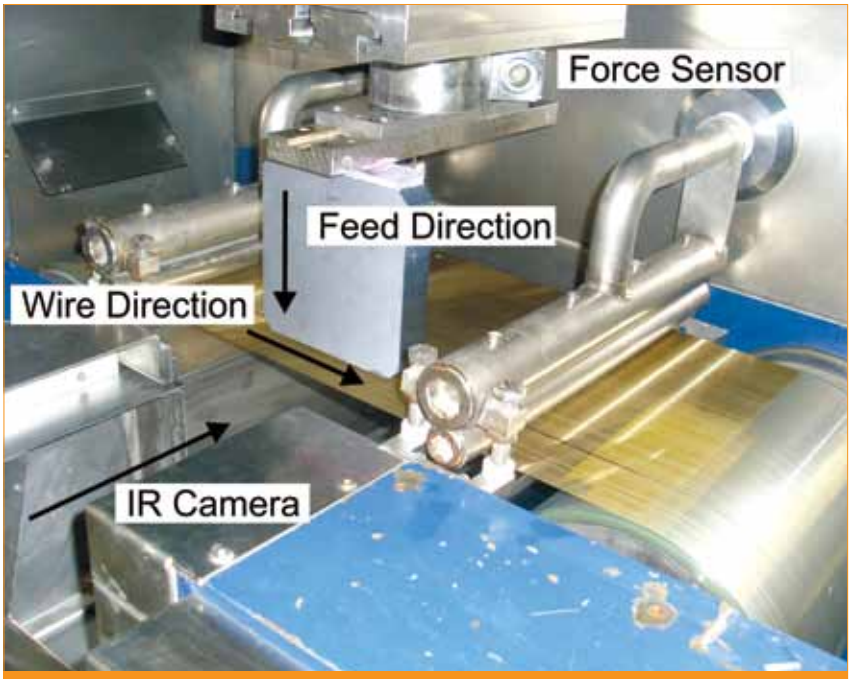

Figure 7. A view into the modified sawing chamber of a Meyer Burger DS 265 wire saw showing slurry nozzles, wire web, feed-in table with mounted force sensor and ingot, and an opening on the side for the infrared camera.

total tension requires the installation of a force sensor between the ingot and its mounting to the saw (Fig. 7). This load cell records the forces during cutting in the wire's direction, the direction of movement of the brick (feed direction), as well as the normal force on the wafer's surface. The force in feed direction is of special interest for the load of the wire; familiarity with this type of force is also essential for a thorough and accurate evaluation of the effectiveness of the sawing process. The force in wire direction describes the friction force and determines the energy loss of the sawing process. An example of such a time-dependent force measurement is given in the graph in Fig. 8, plotted from data gathered from the cutting of a multicrystalline brick with a wafer length of 156mm.

At the beginning of the sawing process, wire and table speeds increase, as does the area of brick that is in contact with the wire, leading to a gradual escalation of the forces at play. Although the force in the wire direction reaches a state of equilibrium within a few minutes, it continues to oscillate at the same frequency as the slurry temperature, which is regulated by a water cooling circuit. In this particular case, the temperature of the slurry that flows out of the slurry nozzles oscillates at an amplitude of about 1 K and over a period of about 7.5 minutes. The force in the wire direction oscillates with the same period and at an amplitude of ±0.05N/(wire·mm). Higher temperatures lead to lower viscosity and hence lower friction in the wire direction.

The force in the feed direction needs time to reach a steady state. This 'bootup' time can take approximately 70 minutes, depending on the wafer size and the feed speed, as the wire bow must be built up. The force exerted by the bow is in equilibrium with the force in the feed direction. As the wires bow down due to the feed, they exert a force upwards. At the end of the process, the wires cut into the mounting glass plate, the wire and table speed are reduced and the forces decrease.

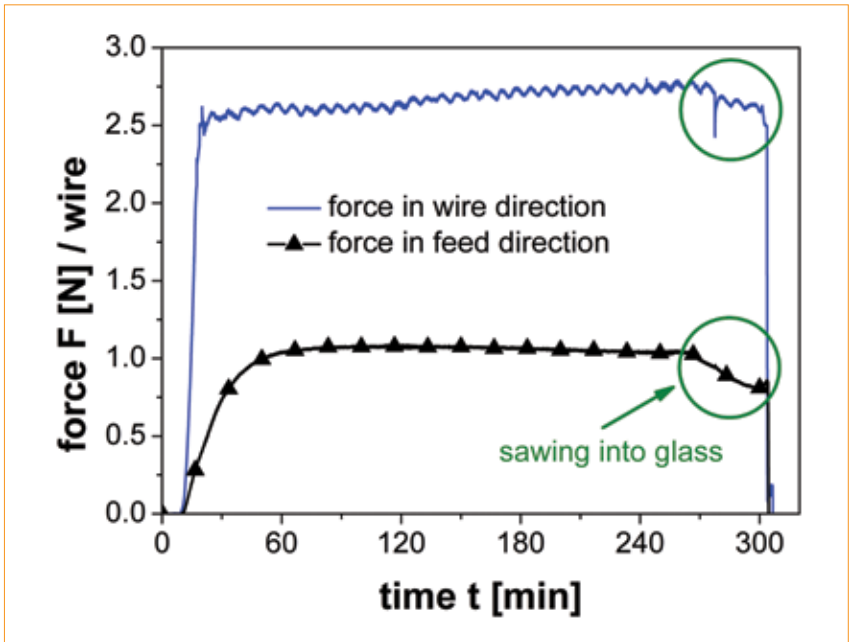

Figure 8. Forces in wire and feed direction measured at the ingot during cutting as a function of time.

Measurements of transient brick temperatures during wire sawing

Equivalent information can also be obtained by observing the increase of brick temperature due to the friction. The temperature on the side face of the ingot is measured with an infrared (IR) camera, which is positioned normal to the wafer surface [5,6].

Fig. 9 shows a typical temperature distribution with a gradual increase of temperature of about 15 K from the wire entrance (left side) to the wire exit (right side). The parameters that influence the removal process also have an effect on the friction in the sawing channel. The forces at play in the wire direction are basically in agreement with the heat development in the brick.

Slurry fluid

The slurry fluid is charged with the responsibility of carrying out several tasks at once. It has to transport the abrasive particles into the sawing channel and the abraded silicon chips out of the sawing channel. In addition, it acts as a removal mechanism for the iron particles that are worn from the wire. For sawing purposes, the SiC particles have to be dispersed homogeneously in the slurry fluid, which in turn transmits the kinetic energy from the wire onto the abrasive particles. The slurry also has to avoid contact between wire and ingot, and thus reduce the lubrication force. Any reduction in the slurry's viscosity lowers the TTV [7]. In contrast, an increase in lubrication force causes an increase in the distance between wire and ingot, as well as an increase in the TTV. Finally, the slurry cools the ingot during sawing.

The slurry viscosity is the main factor behind the internal friction and lubrication in the sawing channel (Fig. 10). Attention must be paid to the process by measuring the forces at play in the wire direction as slurry can splash against the front brick side at the wire inlet, resulting in an additional force on the ingot. This force was subtracted from the total measured force to obtain the net friction force [5]. Preliminary results also show a weaker dependence on slurry viscosity for the forces in the feed direction.

Knowledge of the slurry's temperature is essential for accurate determination of the slurry viscosity in the sawing channel. For instance, the temperature in the sawing channel rises from 33°C at the wire inlet to 47°C at the wire outlet point, as depicted in Fig. 9. This causes a reduction of the slurry viscosity along the wire, which has an impact on the sawing performance (Fig. 10). Although this effect is not completely understood, it is clear that this effect is reduced for a slurry fluid with a lower temperature dependence on the viscosity.

Fig. 11 shows the viscosity of different slurries as a function of temperature. The degree of dependence, depicted by the slope of the curves in the graph, decreases from PEG300 to PEG200 and decreases further for mineral oil. The viscosity of the PEG200/F800 slurry decreases more severely with rising temperatures than does the viscosity of mineral oil/F800 slurry. Between 45°C and 53°C, the viscosities of these two slurries are quite similar.

The slurry viscosity is also dependent on the mass fraction of SiC particles; slurries containing 42 to 49 wt. % of SiC are usually applied. Keeping the mass concentration constant, the slurry viscosity rises significantly for smaller grit sizes (Fig. 12). In practice, finer SiC grit sizes are used to ensure that wafer surface damage is kept

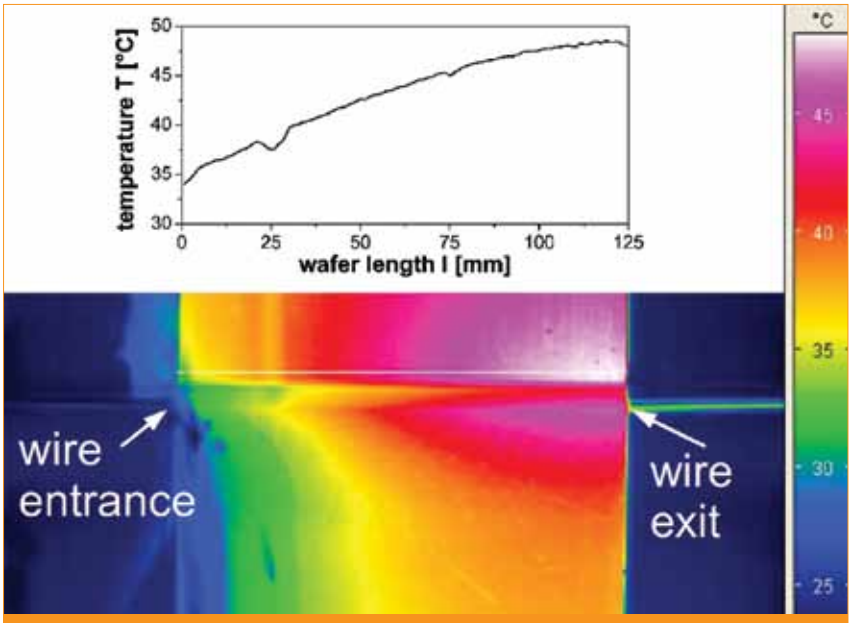

Figure 9. Temperature distribution at the ingot surface measured with an infrared camera.

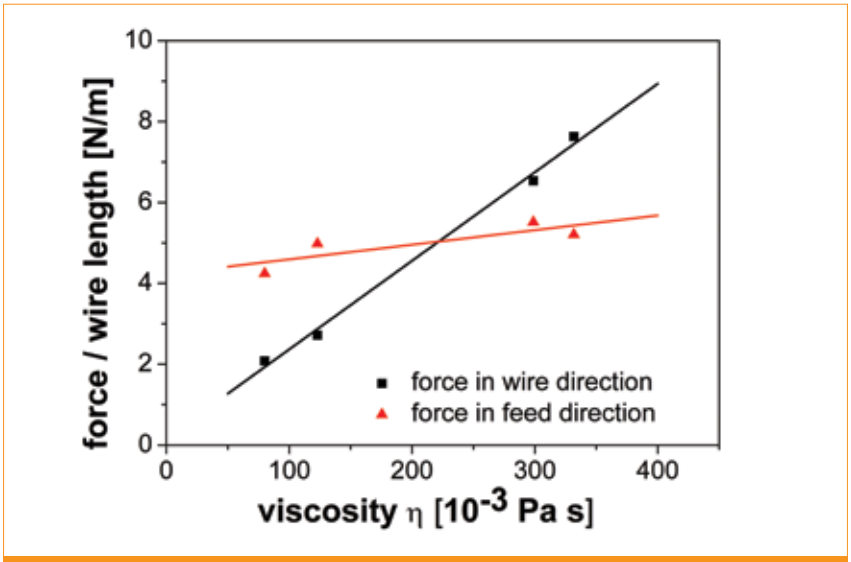

Figure 10. Measured forces per unit wire length during cutting vs. slurry viscosity (at room temperature, for different slurries).

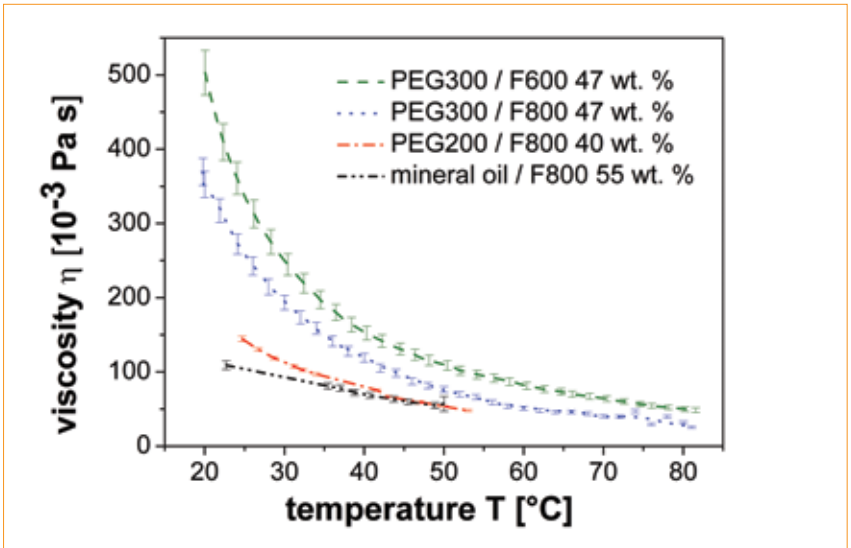

Figure 11. Slurry viscosity vs. temperature.

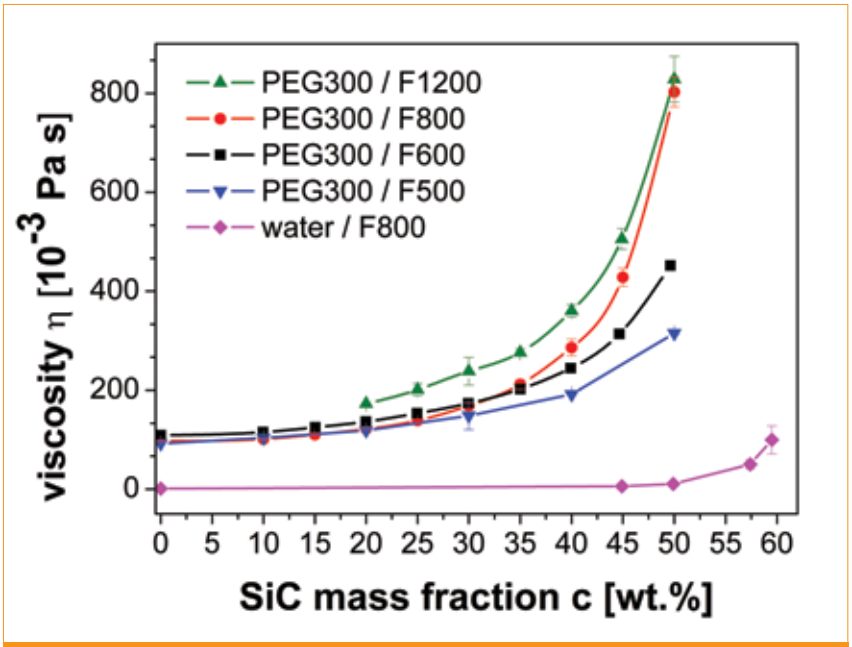

Figure 12. Slurry viscosity vs. SiC mass fraction.

to a minimum – a factor that is especially important when sawing thinner wafers.

However, more energy is needed when using finer grit sizes (Figs. 10 and 12), while the total thickness variation decreases [7,8]. Furthermore, the flow properties of the slurry at room temperature are greatly affected, which might increase the risk of wire breakage. Finally, for reduced grit sizes of SiC, the concentration at which the viscosity diverges is also reduced. Therefore a reduction of SiC content is necessary in order to adjust to the optimum viscosity regime; conversely, an SiC content that is too low reduces the sawing performance such that the optimum performance regime becomes limited.

In addition to the influence of the abrasive concentration and the temperature, the flow characteristic of the slurry also depends on the carrier fluid. The change of the slurry fluid to PEG200, mineral oil or even water is a feasible option to keep the slurry viscosity optimal. The fluid should be optimized in respect to temperature dependence of the viscosity, heat conductivity, surface tension and the difference in density between the carrier fluid and SiC – all of these parameters can influence the sawing process. Nevertheless, the impact of the slurry's properties on the sawing performance is still not completely understood.

Wafer quality

A detailed evaluation of the sawing process would not be complete without a closer look at the wafer's surface quality. Such scrutiny also allows inspectors to draw some conclusions as to the wafer's surface properties and its likely behaviour in regard to the cutting process. It is extremely important to characterize the wafer surface and document any damage accurately.

The wafer surface can be described in terms of its roughness and subsurface damage, while the wafer thickness, total thickness variation (TTV) and the kerf width [8,9] can offer additional information regarding the cutting process.

Cracks are generated by indenting particles. The microcracks, which go from the wafer surface into the body of the wafer, directly determine the wafer stability. These

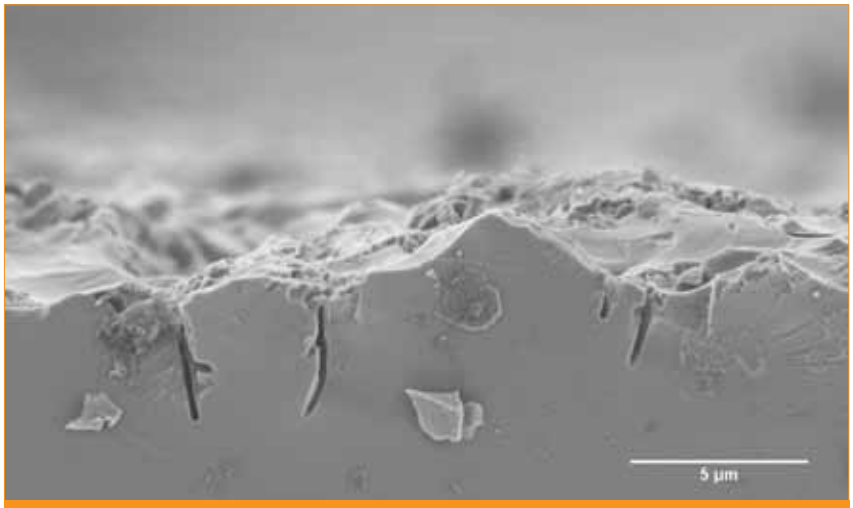

Figure 13. Cleavage edge of an as-cut wafer after etching observed with a scanning electron microscope.

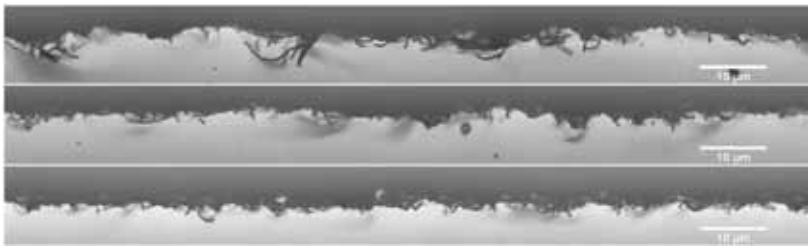

Figure 14. Cleavage edge as observed with a confocal microscope at the wire inlet (top), at the centre of the wafer (middle) and the wire outlet (bottom). Image scope is 120µm × 12µm.

cracks depend on the shape, the size and the indenting force of particles, wire load and wire speed. Several different measurement methods exist that can describe the frequency of cracks, crack depth and fracture stresses of a wafer charge.

Crack investigation at cleaved edges

Access to sharp images of the as-sawn wafer surface and three-dimensional height information are extremely advantageous in the investigation of rough surfaces. To this end, the application of confocal microscope measurements has turned out to be very helpful. Images showing the crack distribution and damaged wafer surface can also be gained by scanning electron microscopy (SEM), as shown in Fig. 13, but investigating a large amount of cracks using this technique would indeed be a tedious task.

The confocal microscope was used to determine the crack size distribution and the crack density of wafer surfaces near the wire inlet and wire outlet on cleaved cross sections of a monocrystalline silicon wafer. Samples were broken into parts and etched by Secco-etching-solution to widen the cracks to allow for better investigation [10], a method that is only applicable to monocrystalline silicon because of the necessity for cleaving. The three images in Fig. 14 show the cleavage edge as observed with a confocal microscope of the wire inlet, middle of the wafer and the wire outlet.

Crack investigation at bevelled surfaces

Another technique developed by TU Bergakademie Freiberg is the characterization of subsurface damage on bevelled polished specimens. The depth distribution of microcracks becomes visible on polished surfaces which are at a slight incline to the original damaged wafer surface [11]. The surfaces are slightly etched to widen the cracks, allowing the calculation of the depth of the microcracks. This method works both for single and multicrystalline silicon.

Fig. 15 shows an example of the coarse section and a detailed view of a bevel polished surface. The bottom part of the left micrograph corresponds to the as-sawn wafer surface. The transition region from the as-sawn surface into the laid-open inside of the wafer is enlarged in the right part of the image. The black thread-like lines are penetrative microcracks; the black areas are indents and pits. By measuring the micrographs and surface profile of the bevel polished surfaces, it is possible to ascertain which crack goes deepest into the volume of the wafer and its depth. The crack depth was measured along the wire direction on bevelled surfaces for different SiC grit

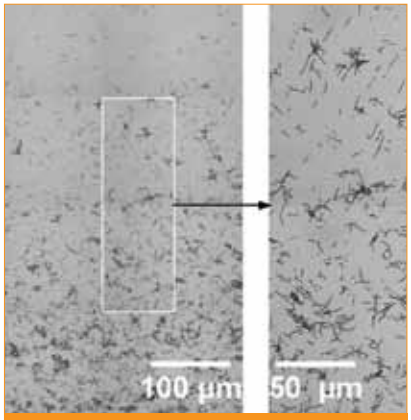

Figure 15. Micrograph of a polished and etched bevel cut.

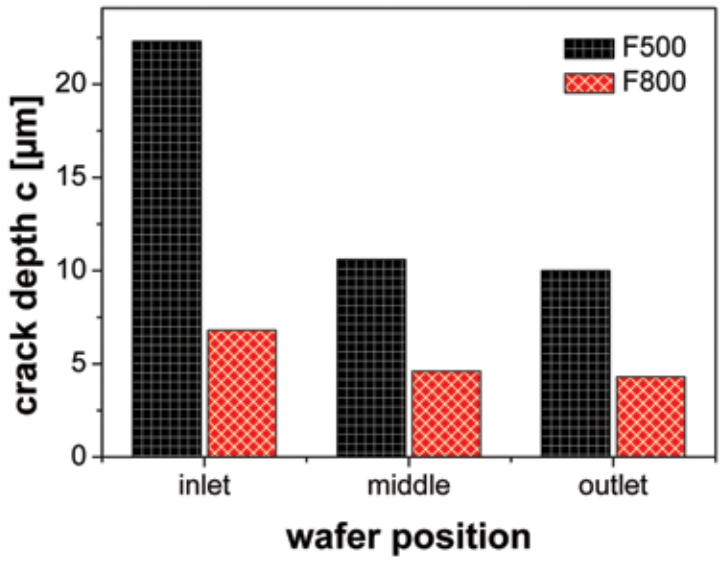

Figure 16. Crack depth as a function of position on the wafer for wafers sawn with different particle size distributions.

sizes leaving the other sawing parameters constant.

Results of crack depth measurements

The distribution of cracks in a wafer is inhomogeneous. Cracks tend to be longer at the wire inlet, decreasing in length towards the wire outlet (Figs. 14 and 16), Furthermore a decrease of roughness can be clearly seen (Fig. 14).

Crack depth results were obtained for wafers sawed with particle size distributions of F500 and F800 (see Fig. 16). Investigations conducted on bevelled surfaces show that the crack depths are strongly influenced by the size distribution of SiC sawing particles. Finer grit sizes reduce the damage depth.

Spatial crack distribution and crack density

Counting the number of cracks along the cleavage edges of the three images in Fig. 14 shows that the number of cracks increases from wire inlet to wire outlet. In order to prove this observation, the crack size distribution and the crack density in a larger area were determined by evaluating several images of 64 × 294µm in size. At least 1mm of cross-sectional sample length has to be measured to ensure a statistically reliable result.

A decrease in the crack size is also to be found in the depth distributions in the form of a shift from deep cracks to shallower ones (Figs. 17 and 18). The local crack density is obtained by counting the total number of cracks (Fig. 19). While the wire inlet features fewer but larger (4.5µm) cracks, the wire outlet tends to generate more numerous but shorter (2.5µm) cracks.

The finding that the fracture stress distribution of a batch of wafers depends not only on crack size but also on the density of the cracks is an extremely important result, and one that is quite often not taken into account. On the one hand, it is necessary to reduce the crack size, but at the same time, the number of cracks induced into the material should not increase. Both size and density of cracks are entered into Weibull statistics [12] and influence the characteristic fracture stress σ_0 (Equation 1).

Mechanical properties

All the experimental results about the microcracks penetrating from the surface of the sawn wafer into the volume confirm that the crack lengths follow a distribution. This crack length distribution is influenced by the grit size of sawing particles, the sawing parameters and possibly the shape of the particles. In addition, the distribution varies over the wafer surface.

Weibull analysis

As silicon is brittle at temperatures lower than 880K [14], these crack length

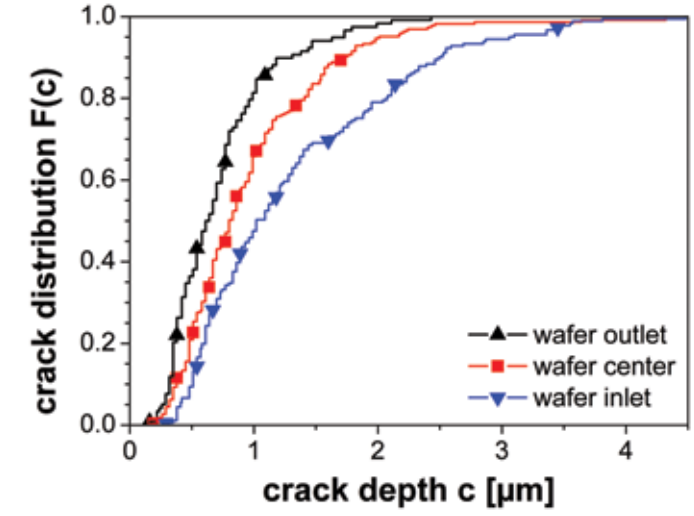

Figure 17. Crack depth distributions F(c) along the cleavage edge at different positions on the wafer's surface.

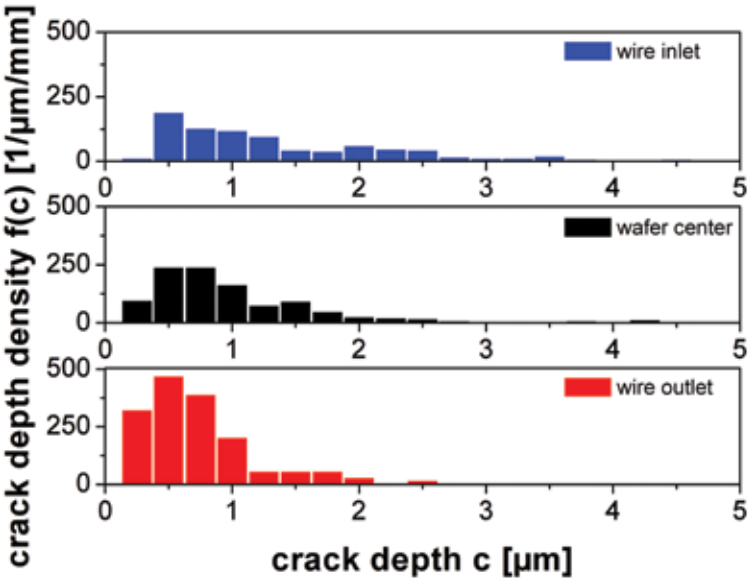

Figure 18. Histogram of the counted crack depths at different positions along the wafer's cleavage edge.

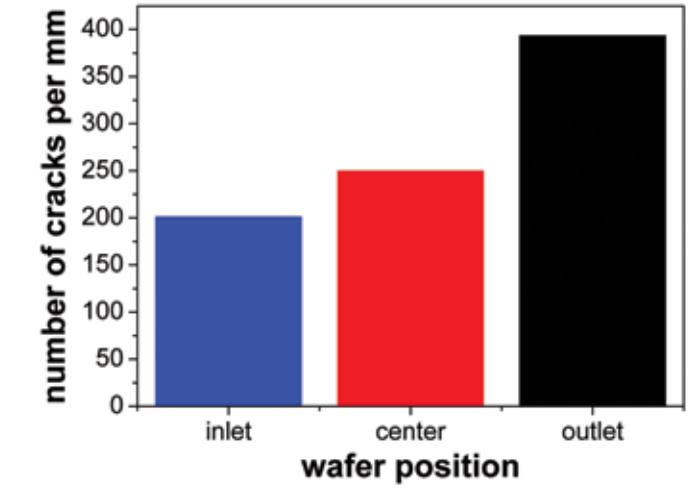

Figure 19. Total number of cracks along the cleavage edge at different positions on the wafer's surface.

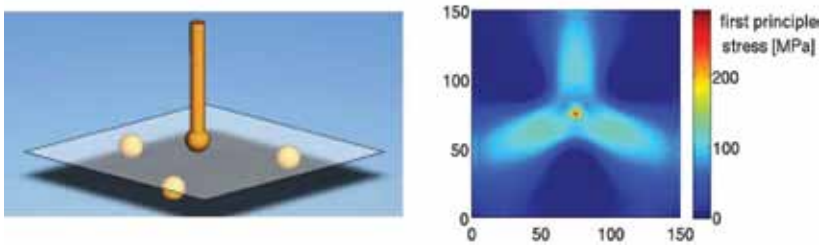

Figure 20. Left: fracture test setup. Right: finite element calculations of stresses generated in a silicon wafer through 5mm displacement in a biaxial fracture test setup (Young's modulus = 165GPa; wafer thickness = 200µm).

distributions are directly responsible for the mechanical properties of the wire-sawn wafer [13]. The 'weakest link', or the longest crack in a loaded wafer, will undoubtedly cause mechanical failure. Brittle fracture of the wafer occurs instantaneously if any crack is loaded with stresses exceeding the strength of that crack. When loading different wafers in a batch of comparable wafers, the fracture stresses will be different for all wafers and will form a fracture stress distribution. Statistical considerations based on the inhomogeneous Poisson process of crack lengths or strength result in the Weibull theory and predict a Weibull distribution of fracture stresses [13]:

$$F(\sigma) = 1 - \exp\left\{-\left(\frac{\sigma}{\sigma_0}\right)^m\right\} \quad (1)$$

Here $F(\sigma)$ is the failure probability ($0 \leq F(\sigma) \leq 1$) for a load σ; σ_0 is the so-called characteristic fracture stress where 63% of all wafers are broken; m is the Weibull parameter that characterizes the width of fracture stress distribution. The higher the Weibull parameter m, the narrower the fracture stress distribution. The characteristic fracture stress σ_0 is a function of the loaded volume [13]. The greater the loaded volume, the higher the probability of there being a crack of critical length in the volume. The tested wafer volume is not changed for a fixed experimental fracture test setup. Thus, σ_0 is a feasible parameter for the comparison of batches of wafers with different mechanical properties.

Weibull plots are graphs that plot the fracture stresses of a batch of wafers in the form $ln\ (ln\ (1/(1- F(\sigma))))$ as a function of $ln(\sigma)$ (or $log\ (ln\ (1/(1-F(\sigma))))$ as a function of $log(\sigma)$). Weibull distributed data plots as straight lines. The Weibull module m is the slope of the line and $m \cdot ln(\sigma_0)$ is the axis intercept. The steeper the line in the graph, the narrower the fracture stress distribution, while lines that tend more towards the left of the graph represent a weaker batch of wafers than those that tend towards the right.

The estimation of Weibull parameters σ_0 and m should be conducted using the 'Maximum-Likelihood' method [15]. Although the tested volume V can be neglected when comparing batches of wafer with the same load test, it plays an important role during the comparison of different fracture test setups.

Depending on the surface type undergoing characterization, there is a variety of different modes of fracture tests available [16]. The biaxial fracture test yields the highest load in the centre of the tested specimen's surface and therefore tests the as-sawn wafer surface [17]. Thus, the biaxial fracture test has been widely used to investigate the impact of wire sawing parameters on mechanical properties of wafers. By cutting the sawn silicon wafers into smaller specimens using a laser beam, this test can even deliver locally resolved fracture stress distributions [18]. A second test set-up uses four-line bending, which exerts a homogeneous stress between the inner bars, both on the surface and on the specimen edges. As long as the cracks on the wafer edges are longer than on the surface (which is frequently the case), this test mainly characterizes fracture properties of the specimen edges between the inner bars. This test can be used to characterize the mechanical stability of the overall wafer,

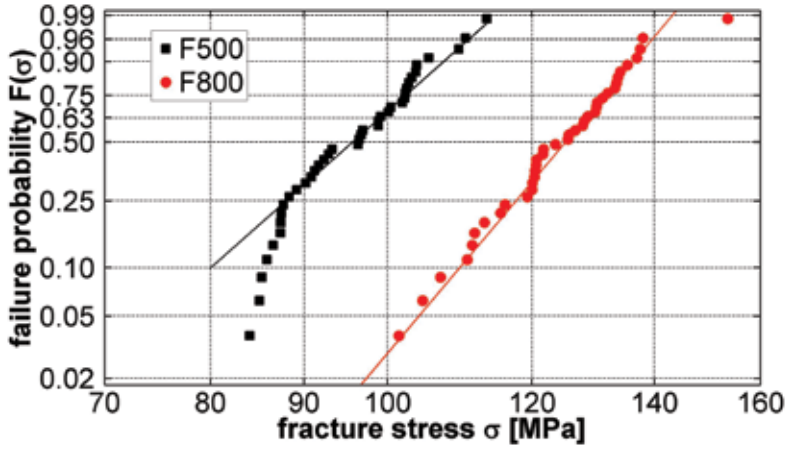

Figure 21. Weibull plot of fracture stress distribution of wire-sawn silicon wafers with varying particle size distribution (sawing parameters: slurry: PEG 300; SiC: 47 wt. %; 14m/s wire speed, 0.6mm/min feed rate.

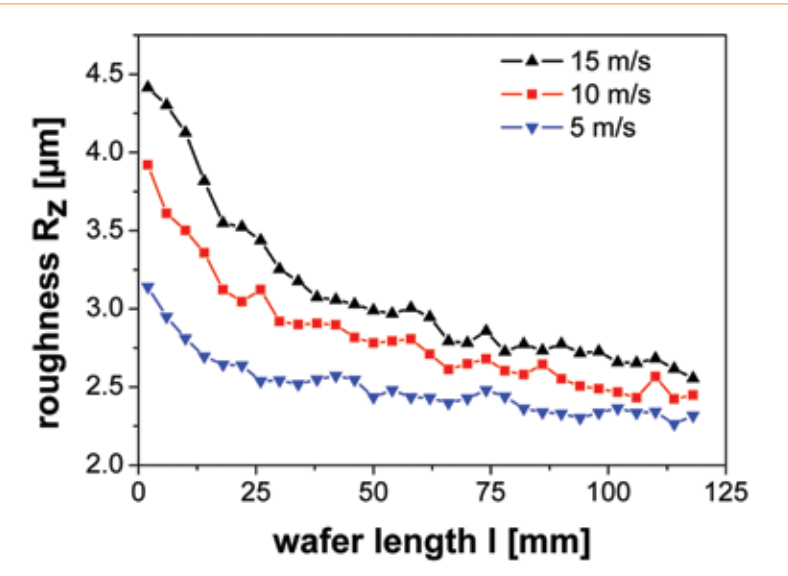

Figure 22. Roughness profiles from wire inlet to wire outlet region for wafers sawn at different wire speeds.

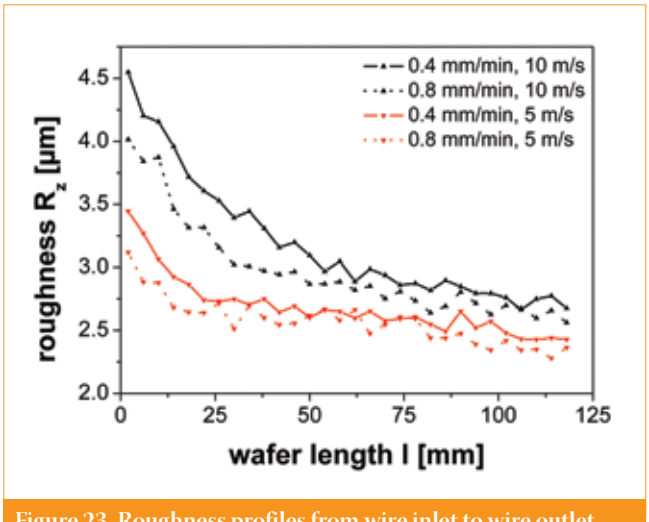

Figure 23. Roughness profiles from wire inlet to wire outlet region for wafers sawn at different wire speeds and feed rates.

including wafer edges, and to check the benefits of the damage etch process [19].

Finite element analysis

Wafer bending tests lead to high deflections of specimens, especially as wafer thicknesses become smaller. In such a case, standard analytical solutions for the calculation of fracture stresses from measured forces are not suitable. Finite element calculations for each wafer geometry and geometrical test setup are required to deduce stress-displacement curves from corresponding measured force-displacement curves [20]. Fig. 20 gives an example of calculated stresses generated in a silicon wafer through displacement in a biaxial fracture test setup.

Fracture test results

The force-displacement curve of Si wafers up to fracture has to be determined in practice. At least 30 to 40 wafers of equal properties should be tested for the statistical Weibull analysis and the determination of the fracture strength distribution [13]. Fig. 21 shows the biaxial fracture test results for batches of wafers sawn with two different SiC-grit size distributions. The line of measured fracture stresses for the F500 sawn wafer lies to the left of the line of measured fracture stresses of the F800 sawn wafers. Thus, the wafer batch sawn with F500 is weaker than the batch of wafers sawn with F800. The F500 wafers show a characteristic fracture stress of σ_0 = (99±3)MPa with a Weibull module of m = 13±3, whereas the results for the F800 wafer are σ_0 = (129±4)MPa where m = 12±3.

Wafer surface – wafer roughness

Aforementioned results have shown that the subsurface damage of a wafer is inhomogeneously distributed. The cracks at the wafer's side, at the point where the wire enters the ingot during sawing, are deeper than at the wire's exit side; similarly, the crack density is higher at the wire exit. Similar patterns are found for wafer roughness, which decreases from wire inlet to wire outlet. Higher wire speeds lead to higher roughness (Fig. 22). The impact of the wire speed at the wire inlet is greater than at the wire outlet.

The surface roughness is less sensitive to the feed rate than to the impact of wire speed. A decrease in the roughness is achieved by increasing the feed rate (Fig. 23). Again, this influence is greater at the wire inlet than at the wire outlet. Roughness (Figs. 22 and 23) and crack depth (Fig. 16) are both functions of the position at the wafer surface, and change in the same way as both parameters originate from the same indentation process during wire sawing.

Our studies have found that the crack depth at the wire inlet depends on the grit size and the sawing parameters, whereas at the wire outlet the crack depth depends mostly on the SiC grit size.

Conclusions

The results presented herein can offer some guidelines for further developments in the wire-sawing process – particularly relevant considering the need for thinner wafers in the future. The issues that are relevant here are the stability of the wafers to obtain high yield in production and the reduction of silicon material, supplies and energy consumption.

High-speed camera investigations have confirmed that sawing occurs as a result of the direct pressure of the wire on the abrasive particles. The largest particles indent into the ingot and cause material removal and microcrack formation on the wafer surfaces. The wafer damage consists of a rough surface and microcracks, which extend into the bulk. It was shown that the saw damage on the wafer surfaces varies and tends to be higher on the side at which the wire entered the sawing channel. On the other hand, the microcrack density increases towards the exit side. Both factors contribute to the fracture strength of the wafers. The saw damage of the wafer edges depends on the ingot side preparation before the wafers are cut and may be higher than on the surfaces.

The inhomogeneous saw damage has to be taken into account when testing the wafer fracture strength. Different parts of the wafer are tested by the various wafer test methods. Since at present no standard test method has been established, care and attention is required when comparing results from different groups.

The surface damage, which occurs mainly at the wire entry side of the wafers, can be reduced by the use of finer grit sizes, but this also increases the forces on the wire. This limits the use of thinner wires at present as it challenges the fracture stresses for wires. Experimentation and analysis has also suggested that there appears to be an optimum grit size for a given wire diameter.

Furthermore, the extent of the saw damage inflicted also depends on sawing parameters, such as wire and feed speed and tension, and can be reduced to some extent by selecting appropriate parameters – however, this can place restrictive limits on the operation windows in production.

The results also show the influence of the slurry, where viscosity appears to be the major factor. Both the forces in the wire direction (friction) and in the feed direction increase with the viscosity, which in turn increases the saw damage and the forces on the wire. The slurry viscosity depends on the viscosity of the base fluid, the solid fraction of the SiC powder, the particle size, and possibly the shape of the powder grains. Since the temperature during sawing varies along the sawing channel, one also has to take into account the temperature dependence of the viscosity. There is also some indication that if the slurry viscosity becomes too low the surface profile develops wider grooves (saw marks) at the wire exit and the risk of wire rupture increases. At present, the best approach to optimizing the slurry parameters remains unclear.

The edge and surface damage occurs at different slicing steps, requiring the application of different strategies in order to improve the overall stability. Considering the wafer surface damage, our results indicate that there may be limitations to producing wafers thinner than 120µm using the presently available materials for wires, carrier fluids and SiC powders.

Acknowledgements

The authors would like to thank Meyer Burger for the generous loan of an industrial wire saw, which enabled them to carry out experiments for over four years. In particular, they want to thank Dr. Fabiano Assi from Meyer Burger, who supported the work and made valuable contributions to the understanding of wire sawing.

References

[1] Möller, H.J. 2004, "Basic Mechanism and Models of Multi-Wire Sawing", *Advanced Engineering Materials*, Vol. 6, No. 7, pp. 501–513.

[2] Kaminski, S. et al. 2010, "The Role of the Slurry Transport in Multi-Wire Sawing of Solar Silicon Wafers", *Proc. 25th EU PVSEC / WCPEC-5*, ISBN 3-936338-26-4, pp. 1312–1317.

[3] FEPA-Standard 2006, "Shapes and Dimensions for Precision Superabrasives", 42–2.

[4] Wagner, T. et al. 2010, "Spatial Distribution of Wafer Subsurface Damage Induced by Wire Sawing", *Proc. 25th EU PVSEC / WCPEC-5*, ISBN 3-936338-26-4, pp. 1267–1271.

[5] Rietzschel, R. et al. 2008, "Optimization of the wire sawing process using force and temperature measurements", *Proc. 23rd EU PVSEC*, ISBN 3-936338-24-8, pp. 1301–1304.

[6] Rietzschel, R. et al. 2010, "Investigation of Polyglycol Based Slurries for Multi Wire Sawing with Lower Forces and Less Hygroscopicity", *Proc. 25th EU PVSEC / WCPEC-5*, ISBN 3-936338-26-4, pp. 1596–1599.

[7] Anspach, O. et al. 2008, "Investigations on Single Wire Cuts in Silicon", *Proc. 23rd EU PVSEC*, ISBN 3-936338-24-8, pp. 1098–1103.

[8] Anspach, O. & Lawerenz, A. 2010, "Understanding the role of abrasives used in the multi-wire sawing process", *Photovoltaics International, 6th Edition*, pp. 36–43.

[9] DIN EN 50513 (VDE 0126-18) 2009, "Solar wafers – Data sheet and product information for crystalline silicon wafers for solar cell manufacturing", Beuth Verlag GmbH, Berlin, Germany.

[10] Secco d'Aragona, F. 1972, "Dislocation Etch for (100) Planes in Silicon", *J. Electrochem. Soc.*, Vol. 119, Issue 7, pp. 948–951.

[11] Funke, C. et al. 2004, "Towards thinner wafers by multi wire sawing", *Proc. 19th EU PVSEC*, pp. 1226–1269.

[12] Wiegand, S. 2003, "Statistische Analysen zur Bruchfestigkeit von Porenbeton und Halbleiterwerkstoffen - Weibull-Theorie und Geostatistik", Diplomarbeit, TU Bergakademie Freiberg.

[13] Munz, D. & Fett, T. 1989, "Mechanisches Verhalten keramischer Werkstoffe", *Springer Verlag*.

[14] Sen, D. et al. 2010, "Atomistic Study of Crack-Tip Cleavage to Dislocation Emission Transition in Silicon Single Crystals", *Physical Review Letters*, PRL 104, pp. 235502-1-235502-4.

[15] DIN 51110 Teil 3, 1993, "Prüfung von keramischen Hochleistungswerkstoffen, 4-Punkt-Biegeversuch, Statistische Auswertung, Ermittlung der Weibull-Parameter".

[16] Funke, C. et al. 2008, "Surface properties of wire sawn wafers", *Proc. 11th Scientific and Business Conference SILICON*, Rožnov pod Radhoštěm, Czech Republic, ISBN 978-80-254-3278-5, pp. 53–58.

[17] Funke, C. et al. 2004, "Biaxial fracture test of silicon wafers", *Adv. ENG. Mater.*, Vol. 6, pp. 594–598.

[18] Orellana Pérez, T. et al. 2010, "Mechanical characterization of epitaxial wafer equivalents from block casting to thin film deposition", *Proc. 25th EU PVSEC / WCPEC-5*, ISBN 3-936338-26-4, 2010, pp. 3619–3625.

[19] Funke, C., Wolf, S. & Stoyan, D. 2009, "Modeling the Tensile Strength and Crack Length of Wire-Sawn Silicon Wafers", *J. Sol. Energy Eng.*, Vol. 131, Issue 1, pp. 011012-1–011012-6.

[20] ANSYS® Multiphysics™, Academic Research, Release 12.1.

About the Authors

Thomas Behm studied applied natural science at the Technische Universität Bergakademie Freiberg. After receiving his diploma in 2007, he began working as a Ph.D. candidate at Prof. H.-J. Möller's photovoltaic research group at the TU Freiberg. His main areas of research are surface and subsurface damage of silicon and sapphire.

Wolfgang Fütterer studied environmental engineering at the TU Bergakademie Freiberg and received his diploma degree in 2004. He then began working as a Ph.D. candidate in Prof. Möller's photovoltaic research group, where his research focuses on the numerical and experimental investigations of the machining process of silicon.

Claudia Funke studied physics at the University of Göttingen, then after conducting studies into metal physics, completed her Ph.D. in 1994 based on investigations into microstructures, orientation changes and the released enthalpy during the recrystallization of Fe-Si alloys. From 1995–97 she worked as a post doc at the Jülich research centre. She joined the TU Freiberg photovoltaic group in 1999.

Steffi Kaminski studied applied natural science at the TU Bergakademie Freiberg. Her diploma thesis investigated optical measurements of surface damage of silicon wafers after mechanical processing. Since 2008, she has been working at the TU Bergakademie as a research scientist on analysis and optimization of the wire sawing process.

Hans-Joachim Möller studied physics at the University of Göttingen, Germany, and received his Ph.D. degree in 1976 on problems of dislocation motion in silicon. In 1982 he became Professor of semiconductor technology at the Technical University of Hamburg-Harburg and in 1994 he took the role of Professor for experimental physics at TU Freiberg in Germany. He then proceeded to build up a research group on photovoltaics with a focus on multicrystalline silicon and related material issues.

Romy Rietzschel studied applied natural science at the TU Bergakademie Freiberg. While working on her diploma thesis in 2006, she studied functional etching of silicon surfaces with HCl at the ISE Freiburg. Since 2007, she has been working as a Ph.D. candidate in Prof. Möller's photovoltaic research group, focussing her study on the optimization of the wire sawing process.

Thomas Wagner studied physics at the Technische Universität Dresden and received his diploma degree in 2004. Since 2006 he has been working on the numerical modelling of the wire saw process as a Ph.D. candidate in Prof. Möller's photovoltaic research group.

Enquiries
Dr. Claudia Funke
TU Bergakademie Freiberg
Institute of Experimental Physics
Leipziger Str. 23
09599 Freiberg
Germany

Tel: +49 3731 39 2084
Fax: +49 3731 30 4313
Email: claudia.funke@physik.tu-freiberg.de
Web: http://www.exphys.tu-freiberg.de